DOI: 10.1111/cgf.12364
Eurographics Conference on Visualization (EuroVis) 2014
H. Carr, P. Rheingans, and H. Schumann
(Guest Editors)

Volume 33 (2014), Number 3

Towards an Unbiased Comparison of CC, BCC, and FCC Lattices in Terms of Prealiasing

Viktor Vad[1], Balázs Csébfalvi[2], Peter Rautek[3], Eduard Gröller[4,5]

[1]Tampere University of Technology, Finland
[2]Budapest University of Technology and Economics, Hungary
[3]King Abdullah University of Science and Technology, Saudi Arabia
[4]Vienna University of Technology, Austria
[5]VRVis Research Center, Austria

Abstract

In the literature on optimal regular volume sampling, the Body-Centered Cubic (BCC) lattice has been proven to be optimal for sampling spherically band-limited signals above the Nyquist limit. On the other hand, if the sampling frequency is below the Nyquist limit, the Face-Centered Cubic (FCC) lattice was demonstrated to be optimal in reducing the prealiasing effect. In this paper, we confirm that the FCC lattice is indeed optimal in this sense in a certain interval of the sampling frequency. By theoretically estimating the prealiasing error in a realistic range of the sampling frequency, we show that in other frequency intervals, the BCC lattice and even the traditional Cartesian Cubic (CC) lattice are expected to minimize the prealiasing. The BCC lattice is superior over the FCC lattice if the sampling frequency is not significantly below the Nyquist limit. Interestingly, if the original signal is drastically undersampled, the CC lattice is expected to provide the lowest prealiasing error. Additionally, we give a comprehensible clarification that the sampling efficiency of the FCC lattice is lower than that of the BCC lattice. Although this is a well-known fact, the exact percentage has been erroneously reported in the literature. Furthermore, for the sake of an unbiased comparison, we propose to rotate the Marschner-Lobb test signal such that an undue advantage is not given to either lattice.

Categories and Subject Descriptors (according to ACM CCS): I.3.3 [Computer Graphics]: Picture/Image Generation—Display algorithms I.4.10 [Image Processing and Computer Vision]: Image representation—Volumetric

1. Introduction

In scientific visualization applications, the input data is usually available as a discrete sampled representation, where the data values are associated to the points of a regular sampling lattice. In order to reproduce the underlying signal also between the lattice points, a reconstruction filtering is necessary, which is basically a convolution of the discrete samples with a continuous convolution kernel. If the original signal is sampled on a certain lattice, its spectrum gets replicated around the points of the dual lattice in the frequency domain. The major goal of the reconstruction is to reproduce the primary spectrum, which is located around the origin, as much as possible, and to get rid of the influence of the replicas that are the so-called aliasing spectra. The convolution filtering in the spatial domain is equivalent to a simple multiplication in the frequency domain by the Fourier transform of the filter kernel. Therefore, the primary spectrum can be perfectly reproduced if an ideal low-pass filer is applied on each lattice. The Fourier transform of the ideal low-pass filter is one at the primary spectrum and zero at the aliasing spectra. However, if the sampling frequency is decreased below the Nyquist limit, the replicas get closer to each other such that the aliasing spectra overlap with the primary spectrum. In this case, a perfect reconstruction is not possible, because the aliasing spectra cannot be filtered even with the ideal low-pass filter. Any filter has to either cut off those high-frequency components of the primary spectrum that are corrupted by the aliasing spectra, or reconstruct the high-frequency components taking the risk of prealiasing. Therefore, it is worthwhile to apply a sampling lattice that minimizes the overlapping. In the literature, the FCC lattice is considered to be optimal in

this sense [KEP08, Ent09, ME10, ME11, MES*11, YE12] if the underlying signal is assumed to be undersampled. However, in this paper, we show that the reduction of the prealiasing effect depends on the sampling frequency, and in a realistic range of the sampling frequency, the FCC lattice is, in fact, optimal just for a narrow interval.

The prealiasing effect has to be distinguished from the postaliasing effect, which stems from the non-ideal frequency-domain behavior of a practical filter. As the ideal low-pass filter is of infinite extent, it is impractical and usually approximated by compact polynomial filters that are efficient to evaluate. However, the frequency response of such a practical filter cannot guarantee that the aliasing spectra are multiplied by zero in the stopband. Therefore, the aliasing spectra also contribute to the reconstructed signal causing postaliasing effects [ML94]. In the literature on volume visualization, the design of filters that minimize the postaliasing artifacts to achieve high image quality is a core topic [ML94, EM06, Csé08b, CD09, Csé10, CD10, Csé13]. One might argue that the reduction of the prealiasing is not a visualization problem and it is more related to data acquisition or tomographic reconstruction, since in the visualization stage it is already too late to do anything against prealiasing. On the other hand, these areas are not researched separately and they intensively influence each other. For example, the optimality of a volumetric data representation can be analyzed not just from the aspects of numerical accuracy or data fidelity but from a visualization point of view as well. Although, in our opinion, the study of the prealiasing effects is as important as that of the postaliasing effects, so far in the visualization literature it has not received the attention that it deserves. Especially in comparative studies evaluating different lattices or reconstruction schemes, it is crucial to clearly separate the prealiasing artifacts from the postaliasing artifacts.

The contributions of this paper are the following:

- We derive the sampling efficiency of the FCC lattice in a comprehensible way. This is important because, in some previous papers [Ent09, ME10, ME11, YE12], this sampling efficiency is by mistake reported to be 27% better than that of the CC lattice. This mistake probably stems from the misinterpretation of the absolute sampling efficiencies derived by Petersen and Middleton [PM62] and Miyakawa [Miy59]. We prove that the FCC lattice performs, in fact, 23% better than the CC lattice in terms of sampling efficiency. Although the ratio of 23% is mentioned in previous papers [QXF*07, VCG12], none of them gives a proof or an explanation. Therefore, we think that our simple and comprehensible proof fills a gap in the literature and as such represents an important contribution.
- Previous experiments [Ent09, ME10, ME11, YE12] on the well-known Marschner-Lobb (ML) signal [ML94] were reported to confirm the superiority of the FCC lattice over the BCC lattice in terms of prealiasing. However, we demonstrate that exactly the opposite can be shown by only changing the orientations of the sampling lattices. This is an important extension of the contributions of Vad et al. [VCG12]. Although they also pointed out that the previous experiments gave an undue advantage to the FCC lattice, they did not analyze the sensitivity of the ML signal to the different orientations of the sampling lattices.
- We propose to carefully use the ML signal for visually comparing different lattices in terms of prealiasing. We recommend that the sampling lattices are rotated in such a way that the prealiasing effect is maximized on each lattice. In this case, the different lattices can be fairly compared regarding their worst-case prealiasing effects.
- For a realistic range of the sampling frequency, we theoretically estimate the prealiasing effect by analytically evaluating the overlapping between the primary spectrum and the nearest and second nearest aliasing spectra. This evaluation shows that the CC, BCC, and FCC lattices are optimal in different ranges of the sampling frequency.

2. Related Work

Practical filters provide different reconstruction quality depending on how accurately they approximate the ideal sinc kernel. To visually compare different filters, Marschner and Lobb introduced a test signal (ML), which is difficult to reconstruct if it is sampled near the Nyquist limit [ML94]. The ML experiments nicely show many important properties of a given filter such as smoothing and postaliasing effects, ringing effect, or the preferred directions in case of an anisotropic reconstruction.

The ML signal is also used for a fundamentally different purpose than it has originally been proposed for, namely, to compare different sampling lattices such as the CC, BCC, and FCC lattices [KEP08, Ent09, ME10, ME11, MES*11, YE12]. The idea of these works is to apply the same sampling density and theoretically equivalent filters on each lattice to visually and quantitatively compare the corresponding reconstructions. It is, however, a challenging task to find truly equivalent filters that do not bias the comparisons. First, filters of the same approximation order were proposed to be applied [EDM04, EVDVM08, KEP08]. Here the major problem is that filters of the same approximation order often behave rather differently even on the same lattice [Csé08b]. This leads to different postaliasing effects, which are difficult to distinguish from the prealiasing effects caused by the sampling lattices themselves. Furthermore, filters of a certain approximation order were missing on certain lattices, such as a fourth-order filter on the FCC lattice. Therefore, filters of the closest approximation order were used, which also biased the comparisons [MES*11]. To remedy this problem, B-spline filters were adapted first to the BCC lattice [Csé08a] and then to the FCC lattice as well [ME10, ME11]. These generalized B-spline filters, which are referred to as

Voronoi splines [ME10], provide not just the same approximation order on the different lattices, but interestingly, their supports cover exactly the same number of lattice points. As theoretically the computational cost of a reconstruction filter is proportional to the size of the given filter, a comparison based on the Voronoi splines seems to be fair. Nevertheless, from a strictly practical point of view, the non-separable Voronoi splines derived for the BCC and FCC lattices are much more expensive to evaluate than the B-splines on the CC lattice, because the evaluation cannot be reduced to lower dimensions as in case of a separable B-spline filter.

Based on the assumption that the original signal is spherically band-limited [TMG01, PM62], probably the most consequent and unbiased comparison is guaranteed if an adaptation of the ideal sinc filter is applied on each lattice. Ye and Entezari [YE12] generalized the sinc filter to arbitrary lattices and applied Lanczos-windowed sinc kernels of approximately the same support size on different lattices. However, for efficiency reasons, they used relatively compact filters, which might also introduce a bias because of their different oversmoothing and postaliasing properties. Oversmoothing and postaliasing stem from the deviation from the ideal passband and stopband behavior, respectively [ML94]. Ideally, the adapted sinc kernels would be the most appropriate for a fair comparison, as theoretically they do not introduce oversmoothing or postaliasing at all. Therefore, the larger is the Lanczos window, the smaller is the bias. Consequently, Vad et al. [VCG12] used very large Lanczos kernels to reduce the bias, and pointed out a very specific property of the classical ML signal, which cannot be expected from real-world data sets. Namely, the spectrum of the ML signal is practically disc-shaped, which results in a bias in favor to FCC sampling. Hossain et al. [HAM11] proposed an alternative test signal which has isosurfaces that are spherically bounded, but it has not been proven so far that its spectrum is truly spherically band-limited. We conclude that no good benchmark is available for fairly comparing CC, BCC, and FCC lattices in terms of prealiasing. Alternatively, practical volumetric data could also be used, but recent CT or MRI scanners do not provide the data on BCC and FCC lattices. Therefore, the BCC and FCC volume representations are usually computed indirectly from high-resolution CC representations. This approach is biased as well, because the applied resampling technique immediately introduces a distortion.

In Section 4, we show that after appropriate rotations the ML signal can be used for an unbiased comparison of CC, BCC, and FCC lattices. Although it is not spherically band-limited as assumed by the theory of optimal regular volume sampling, its disc-shaped spectrum can still be considered as a slice of a truly spherically band-limited spectrum. Therefore, we investigate how a slice of such a spectrum can be rotated in a way that the prealiasing is maximized. Using this approach, we evaluate the prealiasing effects for different sampling lattices.

3. Derivation of the Sampling Efficiencies

3.1. Sampling on the Body-Centered Cubic Lattice

According to the well-known Shannon-Nyquist theory [OS89], a 1D band-limited signal can be perfectly reconstructed from its discrete samples if the sampling frequency is higher than twice the band limit and an ideal sinc filter is used for the continuous reconstruction. The optimality of the BCC lattice is derived from the 3D generalization of this theory [TMG01, PM62]. In 3D, it also has to be considered how the bounding volume of the spectrum is defined. It is a natural assumption that the bounding volume is a sphere, because there is no rational reason to assume any preferred direction in the spectrum of a practical signal. If a spherically band-limited signal is sampled on a certain lattice, its spectrum gets replicated around the points of the dual lattice in the frequency domain. The replicas should not overlap, otherwise the primary spectrum located around the origin cannot be cut with an ideal low-pass filter, that is, the original signal cannot be perfectly reconstructed. On the other hand, the sparsest sampling in the spatial domain can be achieved, if the dual lattice ensures the tightest arrangement of the spherical replicas in the frequency domain. Based on the recently proven Kepler conjecture [Hal98], the best choice for this purpose is the FCC lattice, which is optimal for sphere packing. Since the FCC lattice is the dual of the BCC lattice, for sampling a spherically band-limited 3D signal, the BCC lattice provides the best sampling efficiency in the spatial domain [TMG01, PM62].

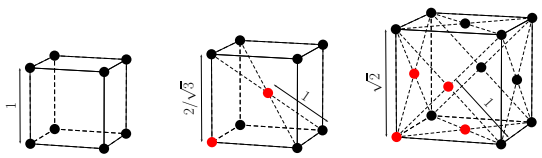

Figure 1: *Dual lattices in the frequency domain corresponding to equivalent CC, FCC, and BCC sampling lattices. (a): Dual CC lattice of a CC sampling lattice. (b): Dual BCC lattice of an FCC sampling lattice. (c): Dual FCC lattice of a BCC sampling lattice.*

Assume that the diameter of the spherical spectrum is one. Thus, the smallest distance between the points of the dual lattice has to be exactly one to achieve the tightest sphere packing in the frequency domain. Figure 1 shows the dual lattices corresponding to CC and BCC sampling, that are CC and FCC lattices, respectively. Note that the dual FCC lattice consists of four overlapping CC lattices (the origins of these CC lattices are depicted by red dots in Figure 1c) with edge length $\sqrt{2}$, so its density (i.e., the number of lattice points per unit volume) is $4/\sqrt{2}^3 = \sqrt{2} \approx 1.4142$. Consequently, the density of the BCC sampling lattice is $1/\sqrt{2} \approx 0.707$, which is 29.3% better than that of the CC lattice [TMG01].

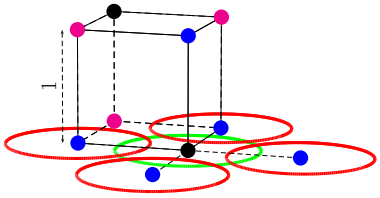

(a) Dual CC lattice corresponding to CC sampling.

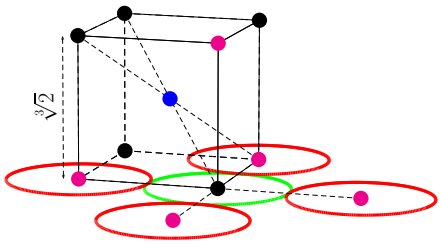

(b) Dual BCC lattice corresponding to FCC sampling.

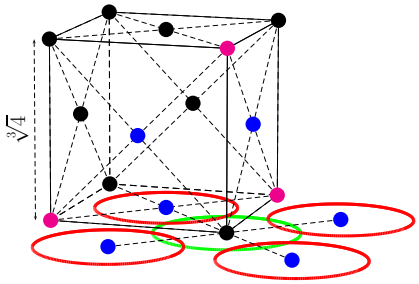

(c) Dual FCC lattice corresponding to BCC sampling.

Figure 2: *Packing of disc-shaped aliasing spectra in the frequency domain on dual CC, BCC, and FCC lattices that correspond to CC, FCC, and BCC sampling lattices of the same density, respectively. The green and red circles represent the primary spectrum and the MS aliasing spectra, respectively.*

3.2. Sampling on the Face-Centered Cubic Lattice

If the original signal is sampled on an FCC lattice then its spectrum is replicated around the points of the dual BCC lattice in the frequency domain. Now let us assume again that the diameter of the spectrum is one. In this case, the smallest distance between the points of the dual BCC lattice has to be exactly one as shown in Figure 1. The dual BCC lattice consists of two CC lattices (the origins of these CC lattices are depicted by red dots in Figure 1b) of edge length $2/\sqrt{3}$. Therefore, its density is $2/(2/\sqrt{3})^3 = \sqrt{3}^3/4 \approx 1.299$. Consequently, the density of the FCC sampling lattice is $4/\sqrt{3}^3 \approx 0.77$, which is 23% better than that of the CC lattice. The gain of 23% is mentioned in previous papers [QXF*07, VCG12] without a proof or an explanation. Those papers that erroneously report the sampling efficiency of the FCC lattice [Ent09, ME10, ME11, YE12] reference the pioneering works of Petersen and Middleton [PM62] and Miyakawa [Miy59], which define the absolute sampling efficiencies of different lattices. This is the reason why we think that the incorrect ratio of 27% might stem from a misinterpretation of their results. Although the relative sampling efficiency of the FCC lattice can also be indirectly obtained from the absolute sampling efficiencies [PM62,Miy59], their derivation is not easy to follow without being familiar with concepts such as the Voronoi cell and the generator matrix of the dual lattice, or the determinant of the generator matrix. In contrast, our proof is simple and relies on minimal background knowledge on sampling lattices. As a consequence, it perfectly serves the goal of resolving the above mentioned contradiction in the literature. We find it important to emphasize that those papers [Ent09, ME10, ME11, YE12] that erroneously report the ratio of 27% provide valuable contributions to the field, which are not invalidated by this mistake.

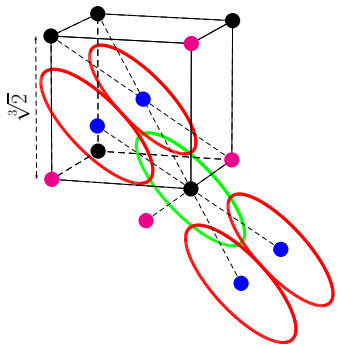

(a) Dual BCC lattice corresponding to a rotated FCC sampling.

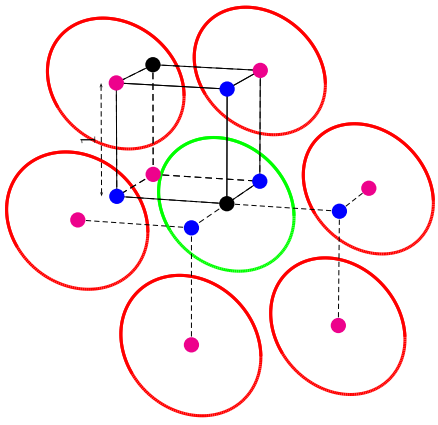

(b) Dual CC lattice corresponding to a rotated CC sampling.

Figure 3: *Packing of disc-shaped aliasing spectra in the frequency domain on dual BCC and CC lattices that correspond to rotated FCC and CC sampling lattices, respectively.*

4. ML Experiments

The ML signal was used in several papers [KEP08, Ent09, ME10, ME11, MES*11, YE12] to visually compare CC, BCC, and FCC volume representations. The experiments in these papers suggest that the FCC sampling ensures lower aliasing than the BCC sampling for undersampled signals. However, recently, Vad et al. [VCG12] demonstrated that the experimental settings were biased. On the other hand, they have not proposed alternative experiments that would lead to an unbiased visual comparison. In this section, we provide additional arguments to justify their statements, namely, we show that the difference in the aliasing effects mainly depends on the orientation of the sampling lattices. Moreover, we show that the ML signal can be used for fair visual comparisons, if it is rotated such that an undue advantage is not given to either lattice. This is a significant extension of the contributions previously published by Vad et al. [VCG12]. Since the spectrum of the ML signal is practically disc-shaped [VCG12], the prealiasing effects depend on how much the primary spectrum overlaps with those nearest aliasing spectra that are in the same plane as the primary spectrum. Therefore, we refer to them as the Most Significant (MS) aliasing spectra of a given plane. Figure 2 shows that the FCC sampling guarantees the largest distance between the primary spectrum and the MS aliasing spectra in the horizontal plane if the sampling densities of the CC, BCC, and FCC lattices are the same and the orientation of each lattice is axis-aligned. In other words, if the MS aliasing spectra get closer to the origin by decreasing the sampling density, the FCC sampling ensures the smallest overlapping in the frequency domain. Note that, in case of CC or BCC sampling, the MS aliasing spectra are located around the dual lattice points that are the nearest neighbors of the origin (these points are depicted in blue in Figure 2). In contrast, in case of FCC sampling, the MS aliasing spectra are located around the second nearest neighbors (these points are depicted in magenta in Figure 2). Therefore, the axis-aligned orientation of the sampling lattices clearly favors the FCC sampling. Table 1 summarizes the distances to the nearest and second nearest neighbors on the dual CC, BCC, and FCC lattices. The distances to the MS aliasing spectra in the horizontal plane are edited in bold.

To make visual comparisons between different reconstructions of the ML signal, we used generalizations of the Lanczos filter as proposed by Ye and Entezari [YE12]. In 1D, the Lanczos filter is defined as follows:

$$L(x) = \begin{cases} sinc(x)sinc(x/a) \text{ if } |x| < a \\ 0 \text{ otherwise,} \end{cases} \quad (1)$$

where $sinc(x) = sin(\pi x)/(\pi x)$. For the CC lattice, a separable tensor-product extension of $L(x)$ is used, while the BCC and FCC lattices require more complicated non-separable extensions [YE12]. Since the ideal low-pass filter can be better approximated by larger filter kernels, we applied extremely large Lanczos filters (parameter a was set to 20) to avoid biased comparisons [VCG12]. On the CC, BCC, and FCC lattices we took approximately the same number of discrete samples, and rendered the corresponding continuous reconstructions by direct isosurface rendering. The images are shown in Figure 4. Similarly to the results of Ye and Entezari [YE12], we also obtained the lowest aliasing effect for the FCC representation of the ML signal. According to their interpretation, the ML experiments confirm the superiority of the FCC lattice over the CC and BCC lattices in terms of antialiasing. Our interpretation is completely different, as we claim that the difference in the prealiasing effects stems from the special shape of the ML spectrum and the orientation of the sampling lattices.

In order to make an unbiased comparison, we have to align the spectrum of the signal with the worst-case scenario of each lattice. We achieve this for sampling the ML signal by rotating the FCC lattice by 45 degrees. This is equivalent by fixing the orientation of the sampling lattice and rotating the ML signal itself, which leads to a different result due to its anisotropic spectrum. In this way, the MS aliasing spectra get to the positions of the first nearest neighbors on the dual BCC lattice (these points are depicted in blue in Figure 3a), which increases the prealiasing effect.

To show the significance of the bias in case of the ML signal, the CC lattice can be rotated such that the MS aliasing spectra get to the positions of the second nearest neighbors (these points are depicted in magenta in Figure 3b), which decreases the prealiasing effect. In this case, we rotate around the z-axis by 45 degrees and then around the y-axis also by 45 degrees. As a result, the axis of the ML signal becomes parallel to the diagonal of the cubic cells. These settings now give an undue advantage to the CC sampling. The corresponding reconstructions are shown in Figure 5. It is clearly apparent that the optimally rotated CC-based reconstruction produces significantly less aliasing artifacts than the worst-case rotated FCC-based reconstruction. We conclude that naive ML experiments are prone to introduce a bias caused by the disc-shaped spectrum of the test signal. Note that the BCC lattice cannot be rotated such that the MS aliasing spectra get to the positions of the second nearest neighbors in the dual FCC lattice. In this case, the aliasing spectra around the first nearest neighbors would be located inside the same plane as the aliasing spectra around the second nearest neighbors. Therefore, the BCC-based reconstruction in Figure 4b can be fairly compared to the FCC-based reconstruction in Figure 5b. Here the MS aliasing spectra are located around the first nearest neighbors on the dual lattices in both cases. In the corresponding images, the BCC representation shows less aliasing than the FCC representation for the worst-case rotation of the sampling lattices.

4.1. RMS Error Measurements

We also measured the RMS errors of the ML reconstructions using an unbiased Monte Carlo estimation. The results sum-

Table 1: *Distances to the nearest and second nearest neighbors on the dual CC, BCC, and FCC lattices.*

spatial domain	CC sampling	FCC sampling	BCC sampling
frequency domain	CC lattice	BCC lattice	FCC lattice
distance to the 1^{st} nearest aliasing spectra	N_{CC} =**1**	$N_{BCC} = \frac{\sqrt{3}}{2}\sqrt[3]{2} \approx 1.0911$	$N_{FCC} = \frac{\sqrt{2}}{2}\sqrt[3]{4} \approx$**1.1225**
distance to the 2^{nd} nearest aliasing spectra	$S_{CC} = \sqrt{2} \approx 1.4142$	$S_{BCC} = \sqrt[3]{2} \approx$**1.2599**	$S_{FCC} = \sqrt[3]{4} \approx 1.5874$

Table 2: *RMS error of the ML reconstruction for different sampling lattices.*

sampling lattice	RMS error
axis-aligned (worst-case orientation) CC	0.0063086
rotated (worst-case orientation) FCC	0.0015537
axis-aligned (worst-case orientation) BCC	0.0012879
rotated (best-case orientation) CC	0.0004630
axis-aligned (best-case orientation) FCC	0.0001718

marized in Table 2 clearly show that the worst-case orientations of the sampling lattices produce much higher error than the best-case orientations. Among the worst-case scenarios, the BCC lattice ensures the highest numerical accuracy. Note that the RMS errors are completely conform to our expectations, since they also demonstrate that the ML signal is very sensitive to the orientation of the sampling lattices due to its anisotropic spectrum.

5. Comparing CC, BCC, and FCC Lattices in Terms of Prealiasing

The previously published ML experiments [KEP08, Ent09, ME10, ME11, MES*11, YE12] clearly showed the lowest prealiasing effect for the FCC representations. These observations easily led to the conclusion that the FCC lattice, in general, minimizes the prealiasing for spherically band-limited signals if sampled below the Nyquist limit. This hypothesis was theoretically explained by the fact that the dual BCC lattice is the best sphere-covering lattice [CSB87], so the FCC sampling ensures the minimal overlapping between the primary spectrum and the nearest aliasing spectra [Ent09]. Another explanation [ME10, ME11, MES*11, YE12] stems from an information-theoretical analysis published by Künsch et al. [KAH05]. It proves that, for sampling stochastic processes, the FCC lattice minimizes the average mean-square error of the best linear interpolation if the sampling frequency tends to zero. Although their framework does not aim at the minimization of the prealiasing effect explicitly, intuitively, the reconstruction error is clearly influenced by the aliasing spectra if the original signal is drastically undersampled. However, as demonstrated in Section 4, when the sampling lattices are rotated such that a bias is avoided, the FCC lattice is not confirmed to be superior over the BCC lattice in terms of prealiasing. This result inspired us to thoroughly investigate the different lattices concerning their prealiasing effects.

In fact, the prealiasing effects can be easily estimated if we take lattices of the same sampling density and gradually increase the diameter of the imaginary spherical spectrum to be reconstructed. In this case, the prealiasing is also gradually increased depending on the increasing overlap between the primary spectrum and the aliasing spectra. This is equivalent to sampling a fixed signal by gradually decreasing the sampling frequency. Note that Figure 2 shows the duals of CC, BCC, and FCC lattices of a unit sampling density, so they contain exactly one lattice point per unit volume. Table 1 shows the distances between the center of the primary spectrum and the centers of the first and second nearest aliasing spectra. The overlap $O(d,t)$ between a spherical primary spectrum and one particular spherical aliasing spectrum depends just on the distance t between them and the diameter d of the spectra. The volume of the intersection between the corresponding two spheres is calculated as follows:

$$O(d,t) = \begin{cases} \frac{1}{12}\pi(2d+t)(d-t)^2 \text{ if } t < d \\ 0 \text{ otherwise.} \end{cases} \quad (2)$$

For the CC, FCC, and BCC sampling lattices, the following equations show the estimated prealiasing effects as the overlapping between the primary spectrum and the nearest and second nearest aliasing spectra depending on their diameter:

$$P_{CC}(d) = 6 \cdot O(d,N_{CC}) + 12 \cdot O(d,S_{CC}), \quad (3)$$

$$P_{FCC}(d) = 8 \cdot O(d,N_{BCC}) + 6 \cdot O(d,S_{BCC}),$$

$$P_{BCC}(d) = 12 \cdot O(d,N_{FCC}) + 6 \cdot O(d,S_{FCC}).$$

Note that, when $d < \sqrt{3} \approx 1.7321$, the third nearest aliasing spectra do not contribute to the prealiasing effect at all on either lattice. Figure 6 shows the estimated total prealiasing effects produced by CC, FCC, and BCC lattices as a function of the relative sampling frequency, which is inversely proportional to the diameter d of the spherical spectrum to be reconstructed. If the sampling frequency is not significantly below the Nyquist limit, the BCC lattice is optimal in terms of prealiasing. In the frequency interval [0.79447, 0.70225], the FCC lattice is optimal. If the signal is drastically undersampled, the traditional CC lattice minimizes the prealiasing effect. Determining the optimality ranges of various lattices is one of the key results of our investigation.

(a) ML signal sampled on an axis-aligned (worst-case orientation) CC lattice.

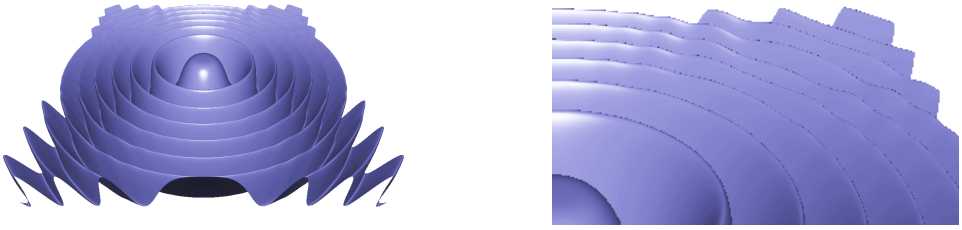

(b) ML signal sampled on an axis-aligned (worst-case orientation) BCC lattice.

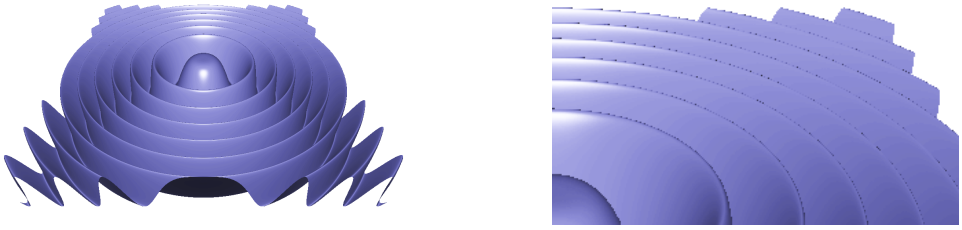

(c) ML signal sampled on an axis-aligned (best-case orientation) FCC lattice.

Figure 4: *Reconstruction of the ML signal from* $40 \times 40 \times 40$ *CC samples (a),* $32 \times 32 \times 32 \times 2$ *BCC samples (b), and* $25 \times 25 \times 25 \times 4$ *FCC samples (c).*

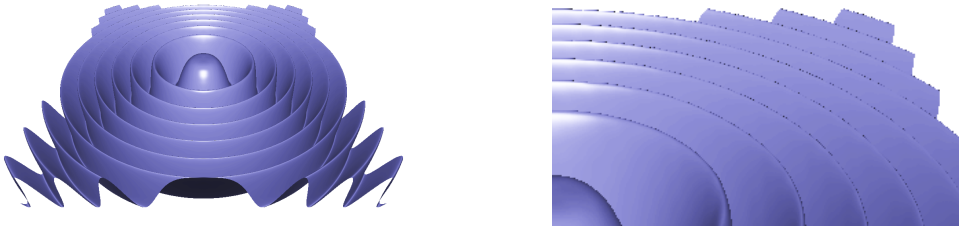

(a) ML signal sampled on a rotated (best-case orientation) CC lattice.

(b) ML signal sampled on a rotated (worst-case orientation) FCC lattice.

Figure 5: *Reconstruction of the ML signal from* $40 \times 40 \times 40$ *CC samples (a) and from* $25 \times 25 \times 25 \times 4$ *FCC samples (b). The sampling lattices are rotated such that the prealiasing is increased on the FCC lattice but decreased on the CC lattice.*

We also evaluated the portion of the primary spectrum which is not corrupted by the aliasing spectra at all depending on the sampling frequency. As shown in Figure 7, in this sense, the CC lattice is clearly the worst choice, while the BCC and FCC lattices perform quite similarly just as according to our prealiasing measure.

Künsch et al. [KAH05] have analytically proven that, using Kriging interpolation on stationary stochastic processes, the average mean-square error is minimized by the BCC and FCC lattices if the sampling frequency tends to infinity and zero, respectively. Our prealiasing estimation is not contradictive to these results. Concerning the BCC sampling, Figure 6 also confirms that the BCC lattice is optimal for high-frequency sampling. Regarding low-frequency sampling, we investigated a realistic interval of the sampling frequency, assuming that practical signals are usually not sampled very drastically below the Nyquist limit. Otherwise, the reconstruction would introduce so much error anyway that the results would not be reliable at all. Therefore, the fact that the FCC lattice minimizes the average mean-square error if the sampling frequency tends to zero [KAH05], does not necessarily mean that the FCC sampling guarantees the lowest prealiasing effect for a realistic sampling frequency.

6. Performance Considerations

In the field of optimal regular volume sampling, papers can be classified to two different categories. The first category is represented by papers that point out the theoretical advantages of non-Cartesian lattices including a better sampling efficiency, reduced aliasing, or a more isotropic volume representation [Miy59, PM62, ME10, YE12, VCG12]. Here the major goal is to demonstrate the superior potential of the BCC and FCC volume representations themselves regardless of the increased complexity of non-separable reconstruction filters. In contrast, papers belonging to the second category aim at efficient GPU implementations that can utilize the theoretical advantages in practice [CH06, FEVDVM10, DC10, DC11, Csé13]. This paper clearly corresponds to the first category. We used very large Lanczos filters because, according to the state of the art, they introduce the least bias [YE12] in our quantitative and qualitative comparisons. However, we consider these large filters as theoretical rather than practical tools. Therefore, we did not measure their performance. In this paper, we intended to clarify the theory of optimal regular volume sampling rather than to propose efficient filters. However, we think that our results should certainly be taken into account when in future works practical non-Cartesian reconstruction schemes are proposed, analyzed, or compared to Cartesian reconstruction schemes in terms of numerical accuracy and visual quality. Recently, promising reconstruction techniques [FEVDVM10, DC11, Csé13] have been published that provide just slightly worse performance compared to that of the most popular CC-based techniques. Nevertheless, to decide between CC, BCC, and FCC representations not just the rendering speed counts but also numerical and visual quality, which in our opinion should be compared as fairly as possible.

7. Conclusion

The major goal of this paper was to refine the interpretation of the prealiasing effects caused by different sampling lattices. By intention, we presented our contributions without complicated mathematical formalizations to make them comprehensible even without thoroughly studying the literature on optimal regular volume sampling.

Previous work [KEP08, Ent09, ME10, ME11, MES*11, YE12] has argued that the FCC lattice minimizes the prealiasing effect if the underlying signal is assumed to be spherically band-limited and sampled below the Nyquist limit. In this paper, the CC, BCC, and FCC lattices have been shown to minimize the prealiasing effect for different ranges of the sampling frequency. Previously, the superior antialiasing effect of the FCC lattice was explained by the fact that its dual BCC lattice is the best sphere-covering lattice [Ent09]. This explanation implicitly assumes that only the nearest aliasing spectra contribute to the prealiasing effect. We have shown that, in case of FCC sampling, the influence of the second nearest aliasing spectra should also be taken into account, as they are relatively close to the primary spectrum. The antialiasing property of the FCC lattice was investigated in several papers [KEP08, Ent09, ME10, ME11, MES*11, YE12] using the well-known ML signal. We have pointed out that, due to its anisotropic spectrum, the results very much depend on the orientations of the sampling lattices. Therefore, we proposed to rotate the sampling lattices such that the prealiasing is maximized on each lattice. Following this approach, the ML signal can be used for an unbiased visual comparison of different lattices.

Overall, according to our results, a volumetric data representation is difficult to optimize by choosing the most appropriate sampling lattice if the data is assumed to be undersampled. As the different lattices are expected to minimize the prealiasing error in different ranges of the sampling frequency, the preferred lattice needs to be predicted somehow based on the given sampling frequency. Nevertheless, the band limit of the original signal is usually not known in advance, so it is hard to decide whether the actual sampling frequency is inside the optimality range of a specific lattice. On the other hand, if the major goal is to maximize that portion of the primary spectrum which is not corrupted by the aliasing spectra at all, the BCC and FCC lattices clearly outperform the traditional Cartesian lattice.

Acknowledgements

This work was supported by the KAUST Visual Computing Center and OTKA K-101527.

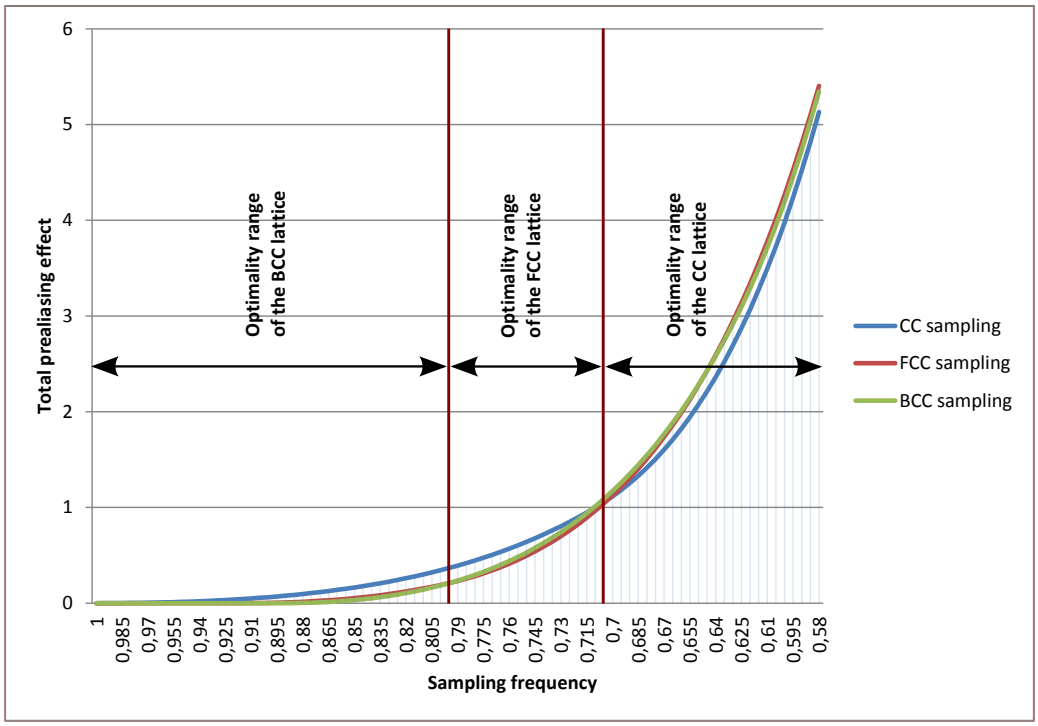

Figure 6: *Estimated total prealiasing effect produced by CC, FCC, and BCC lattices depending on the sampling frequency.*

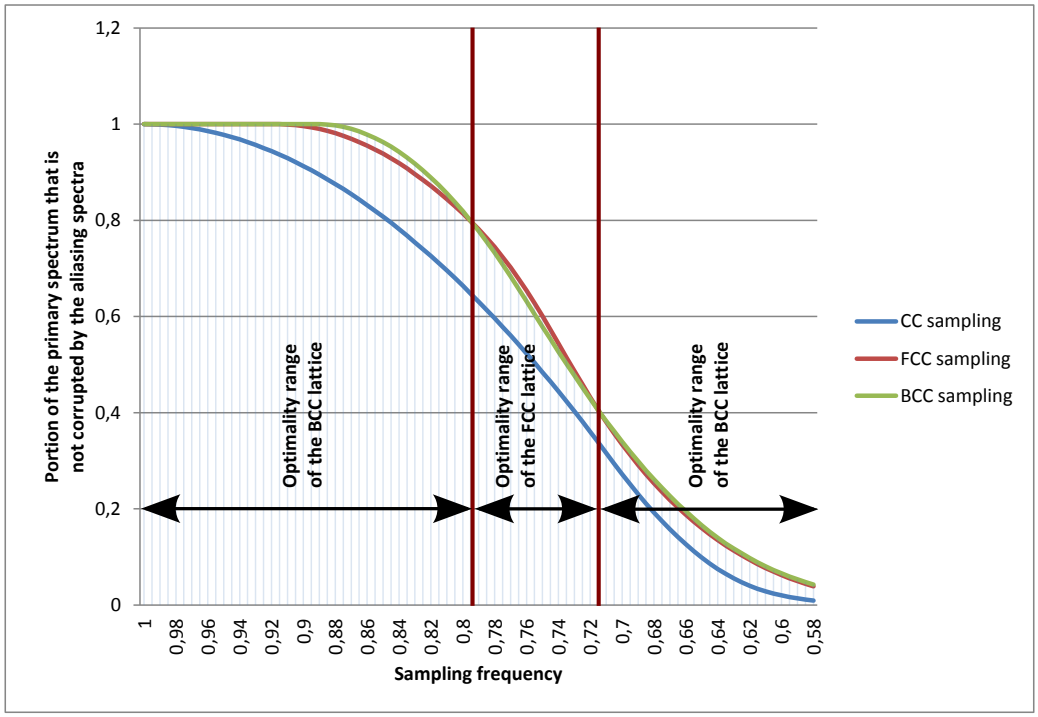

Figure 7: *Portion of the primary spectrum that is not corrupted by the aliasing spectra depending on the sampling frequency.*

References

[CD09] CSÉBFALVI B., DOMONKOS B.: Interactively controlling the smoothing and postaliasing effects in volume visualization. In *Proceedings of Spring Conference on Computer Graphics (SCCG)* (2009), pp. 129–136. 2

[CD10] CSÉBFALVI B., DOMONKOS B.: 3D frequency-domain analysis of non-separable reconstruction schemes by using direct volume rendering. In *Proceedings of Spring Conference on Computer Graphics (SCCG)* (2010), pp. 51–60. 2

[CH06] CSÉBFALVI B., HADWIGER M.: Prefiltered B-spline reconstruction for hardware-accelerated rendering of optimally sampled volumetric data. In *Proceedings of Vision, Modeling, and Visualization* (2006), pp. 325–332. 8

[CSB87] CONWAY J. H., SLOANE N. J. A., BANNAI E.: *Sphere-packings, lattices, and groups*. Springer-Verlag New York, Inc., 1987. 6

[Csé08a] CSÉBFALVI B.: BCC-splines: Generalization of B-splines for the body-centered cubic lattice. *Journal of WSCG 16*, 1–3 (2008), 81–88. 2

[Csé08b] CSÉBFALVI B.: An evaluation of prefiltered reconstruction schemes for volume rendering. *IEEE Transactions on Visualization and Computer Graphics 14*, 2 (2008), 289–301. 2

[Csé10] CSÉBFALVI B.: An evaluation of prefiltered B-spline reconstruction for quasi-interpolation on the body-centered cubic lattice. *IEEE Transactions on Visualization and Computer Graphics 16*, 3 (2010), 499–512. 2

[Csé13] CSÉBFALVI B.: Cosine-weighted B-spline interpolation: A fast and high-quality reconstruction scheme for the body-centered cubic lattice. *IEEE Transactions on Visualization and Computer Graphics 19*, 9 (2013), 1455–1466. 2, 8

[DC10] DOMONKOS B., CSÉBFALVI B.: DC-splines: Revisiting the trilinear interpolation on the body-centered cubic lattice. In *Proceedings of Vision, Modeling, and Visualization* (2010), pp. 275–282. 8

[DC11] DOMONKOS B., CSÉBFALVI B.: Evaluation of the linear box-spline filter from trilinear texture samples: A feasibility study. *Journal of WSCG 19*, 2 (2011), 77–84. 8

[EDM04] ENTEZARI A., DYER R., MÖLLER T.: Linear and cubic box splines for the body centered cubic lattice. In *Proceedings of IEEE Visualization* (2004), pp. 11–18. 2

[EM06] ENTEZARI A., MÖLLER T.: Extensions of the Zwart-Powell box spline for volumetric data reconstruction on the Cartesian lattice. *IEEE Transactions on Visualization and Computer Graphics 12*, 5 (2006), 1337–1344. 2

[Ent09] ENTEZARI A.: Uniform sampling and reconstruction of trivariate functions. In *Proceedings of SAMPTA* (2009). 2, 4, 5, 6, 8

[EVDVM08] ENTEZARI A., VAN DE VILLE D., MÖLLER T.: Practical box splines for reconstruction on the body centered cubic lattice. *IEEE Transactions on Visualization and Computer Graphics 14*, 2 (2008), 313–328. 2

[FEVDVM10] FINKBEINER B., ENTEZARI A., VAN DE VILLE D., MÖLLER T.: Efficient volume rendering on the body centered cubic lattice using box splines. *Computers & Graphics 34*, 4 (2010), 409–423. 8

[Hal98] HALES T. C.: Cannonballs and honeycombs. *AMS 47*, 4 (1998), 440–449. 3

[HAM11] HOSSAIN Z., ALIM U. R., MÖLLER T.: Towards high quality gradient estimation on regular lattices. *IEEE Transactions on Visualization and Computer Graphics 17*, 4 (2011), 426–439. 3

[KAH05] KÜNSCH H. R., AGRELL E., HAMPRECHT F. A.: Optimal lattices for sampling. *IEEE Transactions on Information Theory 51*, 2 (2005), 634–647. 6, 8

[KEP08] KIM M., ENTEZARI A., PETERS J.: Box spline reconstruction on the face-centered cubic lattice. *IEEE Transactions on Visualization and Computer Graphics 14*, 6 (2008), 1523–1530. 2, 5, 6, 8

[ME10] MIRZARGAR M., ENTEZARI A.: Voronoi splines. *IEEE Transactions on Visualization and Computer Graphics 58*, 9 (2010), 4572–4582. 2, 3, 4, 5, 6, 8

[ME11] MIRZARGAR M., ENTEZARI A.: Quasi interpolation with Voronoi splines. *IEEE Transactions on Visualization and Computer Graphics 17*, 12 (2011), 1832–1841. 2, 4, 5, 6, 8

[MES*11] MENG T., ENTEZARI A., SMITH B., MÖLLER T., WEISKOPF D., KIRKPATRICK A. E.: Visual comparability of 3D regular sampling and reconstruction. *IEEE Transactions on Visualization and Computer Graphics 17*, 10 (2011), 1420–1432. 2, 5, 6, 8

[Miy59] MIYAKAWA H.: Sampling theorem of stationary stochastic variables in multidimensional space. *J. Inst. Electron. Commun. Eng. Jpn. 42*, 2 (1959), 421–427. 2, 4, 8

[ML94] MARSCHNER S., LOBB R.: An evaluation of reconstruction filters for volume rendering. In *Proceedings of IEEE Visualization* (1994), pp. 100–107. 2, 3

[OS89] OPPENHEIM A. V., SCHAFER R. W.: *Discrete-Time Signal Processing*. Prentice Hall Inc., Englewood Cliffs, 2nd edition, 1989. 3

[PM62] PETERSEN D. P., MIDDLETON D.: Sampling and reconstruction of wave-number-limited functions in n-dimensional Euclidean spaces. *Information and Control 5*, 4 (1962), 279–323. 2, 3, 4, 8

[QXF*07] QIU F., XU F., FAN Z., NEOPHYTOU N., KAUFMAN A., MUELLER K.: Lattice-based volumetric global illumination. *IEEE Transactions on Visualization and Computer Graphics 13*, 6 (2007), 1576–1583. 2, 4

[TMG01] THEUSSL T., MÖLLER T., GRÖLLER M. E.: Optimal regular volume sampling. In *Proceedings of IEEE Visualization* (2001), pp. 91–98. 3

[VCG12] VAD V., CSÉBFALVI B., GABBOUJ M.: Calibration of the Marschner-Lobb Signal on CC, BCC, and FCC Lattices. In *Proceedings of EuroVis* (2012), pp. 19–23. 2, 3, 4, 5, 8

[YE12] YE W., ENTEZARI A.: A geometric construction of multivariate sinc functions. *IEEE Transactions on Image Processing 21*, 6 (2012), 2969–2979. 2, 3, 4, 5, 6, 8